X-ray radiation effects in multilayer epitaxial graphene

Jeremy Hicks[1], Rajan Arora[2], Eleazar Kenyon[2], Partha S. Chakraborty[2], Holly Tinkey[1], John Hankinson[1], Claire Berger[1,3], Walt A. de Heer[1], Edward H. Conrad[1], and John D. Cressler[2,a)]

[1] School of Physics, Georgia Institute of Technology, Atlanta, GA 30332

[2] School of Electrical and Computer Engineering, Georgia Institute of Technology

[3] CNRS-Institut Néel, Grenoble, France

Abstract

We characterize multilayer graphene grown on C-face SiC before and after exposure to a total ionizing dose (TID) of 12 Mrad(SiO_2) using a 10 keV X-ray source. While we observe the partial peeling of the top graphene layer and the appearance of a modest Raman D-peak, we find that the electrical characteristics (mobility, sheet resistivity, free carrier concentration) of the material are mostly unaffected by radiation exposure. Combined with X-ray photoelectron spectroscopy (XPS) data showing numerous carbon-oxygen bonds after irradiation, we conclude that the primary damage mechanism is through surface etching from reactive oxygen species created by the X-rays.

[a)] Electronic mail: cressler@ece.gatech.edu

Graphene has recently made great strides as a high-performance electronic material [1], with several groups demonstrating devices for potential radio-frequency (RF) applications [2-4]. Like other carbon allotropes, graphene is appealing as a radiation-hardened material, owing to its low atomic number and consequent low capture cross section. Epitaxial graphene grown from silicon carbide (SiC) has the added advantage of being naturally integrated with a wide-bandgap semiconductor, reducing the potential effects of particle-induced substrate damage. Together, these factors suggest that epitaxial graphene is an attractive material for use in electronics for radiation-rich environments.

In this study, we focus on the effects of X-rays, which are typically not energetic enough to cause direct lattice damage, but may create other long-term defects such as charge traps [5]. Prior studies of high-energy photon dose effects in single-walled carbon nanotubes (SWCNTs), a graphene derivative, have suggested that effects extrinsic to the SWCNTs, such as increased impurity adsorption and the formation of oxide traps, are the main cause of changes in FET device properties [6,7]. By contrast, Zhou *et al.*, concluded that even soft X-rays are enough to perturb the sp^2 bond structure of graphene that is weakly-bound to a substrate but that epitaxial graphene on SiC (0001) is largely unaffected [8].

Epitaxial graphene samples in the present investigation were grown at 1550 °C from insulating 4H-SiC $(000\bar{1})$, using the confinement-controlled sublimation (CCS) method, which involves using an enclosure to limit the rate of silicon sublimation from the SiC surface [9]. The average sample thickness was measured by ellipsometry to be 7 layers. Half of each 3.5 x 4.5 mm sample was patterned into several 8-armed Hall Bar structures while the other half was left with bulk epitaxial graphene for characterization by X-ray photoelectron spectroscopy (XPS, $h\nu \approx 1.5$ keV) and Raman spectroscopy ($\lambda \approx 532$ nm). Prior to any measurements, the samples were

cleaned with 10 cc/s of forming gas (3% H_2, 97% Ar) at 250 °C for 3 hours to eliminate photoresist residue. Irradiation was carried out in air in an Aracor 4100 X-ray irradiator, which is equipped with a tungsten source ($h\nu \approx 10$ keV), at a dose rate of 31.5 krad (SiO_2)/min to a total ionizing dose (TID) of 12 Mrad(SiO_2). We note that a TID of 12 Mrad(SiO_2) is significantly larger than that encountered in most orbital applications, and thus it can be considered a worst case exposure for most space systems.

After irradiation, we found in many samples that the graphene had partly peeled, exemplified by the faint depressed region seen in atomic force microscopy (AFM) of a Hall bar (dashed lines) structure in Fig. 1(b). Regions of high topography, pointed to by arrows, suggest that narrow strips of graphene have been cut from the surface and have rolled up like a scroll. A height profile of this region before and after irradiation, shown in Fig. 1(c), suggests that the top layers have peeled, although the exact number of sheets cannot be determined from AFM due to X-ray induced chemical changes in the top layer (differences in material properties are well-known to affect the apparent height of objects at the atomic scale in AFM [10]).

Interestingly, Fig. 1(d), which shows the electrical transport characteristics, measured by average resistivity and carrier mobility/concentration using various arms of Hall bar structures, are essentially unchanged despite obvious physical damage to the surface. Specifically, we found the median carrier mobility/concentrations to be 3% lower each while the median resistivity were 4% higher after irradiation – changes that we consider statistically insignificant given the spread in the data points. Prior to irradiation, the 4 samples were of varying quality, with resistivities ranging from 100-800 Ω/sq, mobilities from 400-4000 cm^2/V-s, and carrier concentrations from 1-3×10^{13} cm^{-2}. The properties of the Hall bars on a particular sample, however, were relatively

uniform. We observed the same unchanged electrical properties in each individual sample regardless of quality.

The seemingly-conflicting electrical and topographical observations presented here can be reconciled by the supposition that the observed peeling does not affect the bottom-most graphene layers. It is well-known that the epitaxial graphene layers closest to the SiC are highly-doped [11,12], and it was stated in the former reference that transport should be dominated by those closest layers as a result. Although this statement, which essentially says that the most conductive graphene layers should dominate the film's electrical properties, is intuitive, it has been difficult to confirm directly. By our supposition, despite either constricting or severing the electrical transport of the top graphene layers after irradiation, there is a minimal effect on the film's electrical properties. We conclude, therefore, both that the bottom-most layers were unaffected by the irradiation and that they further dominate the electrical transport in the film, making our results a direct confirmation of the statement made in Reference [11].

Raman spectroscopy of the samples after irradiation in Fig. 2(a) shows the appearance of small D and D' peaks around 1350 cm^{-1} and 1620 cm^{-1}, respectively, indicating that a small number of edges were created in the graphene lattice [13,14]. The spectrum otherwise has features typical of multilayer graphene such as a single-component 2D peak with a FWHM of 30 cm^{-1} located near 2700 cm^{-1} [15]. Aside from the typical spot-to-spot variations in a single sample, we noted no shifts or broadening of either the G (1570 cm^{-1}) or 2D (2700 cm^{-1}) peaks after irradiation.

C1s XPS data in Fig. 2(b) reveals that the graphene peak (284.5 eV) has widened by about 20% (1.1 eV to 1.3 eV, FWHM) after irradiation. Beforehand, the C1s spectrum was well-described by only two symmetric Lorentzian peaks: one for graphene (284.5 eV) and one for SiC (282.1

eV). In our case, the energy bandwidth of the X-ray beam largely determined the widths of the peaks. After irradiation, the graphene peak became asymmetric, which we found can be represented by adding a new symmetric peak at 285.3 eV to reflect surface damage [16]. Although it is not shown, rigid shifts to higher binding energy of 0.5 to 1.5 eV were observed in the spectra of all samples due to work function changes at the surface. We note that this data is far more surface-sensitive than the Raman data in Fig. 2(a); we estimate from the intensity ratio between the C1s SiC and graphene peaks that the mean photoelectron escape depth is only about 1.5 nm. In addition to the graphene being peak asymmetric, a broad shoulder extending from it to 290 eV formed, which we took to be the sum of three non-graphitic peaks centered at around 286 eV, 287.5 eV, and 288.9 eV. These peaks have been commonly attributed to particular carbon-oxygen bond configurations, namely C–O, C=O, and –COO, respectively, and have been seen after subjecting CNTs to strong oxidation reactions [17,18]. Based on the reported stability of epitaxial graphene to soft X-rays in vacuum [8], we conclude that these oxygen functional groups were created during irradiation rather than after irradiation. In light of this, the peeling seen in Fig. 1(b) is likely mediated by reactive oxygen species that form when subjecting ambient O_2 to X-rays.

In summary, we have irradiated multilayer epitaxial graphene samples grown from SiC $(000\bar{1})$ with a TID of 12 Mrad(SiO_2). While we find that the topmost layer or two has partly peeled away due to X-ray-assisted oxygen etching in air, the impact to carrier transport is small because the charge transport is dominated by layers far from the surface. These results suggest that epitaxial graphene could well be suitable for ionizing radiation environments through the use of a capping layer to prevent radiation-induced oxidation.

The authors would like to thank R. D. Schrimpf for access to X-ray irradiation facilities as well as J. Palmer and C. Johnson for graphene cleaning and characterization assistance. This work as supported in part by the W. M. Keck Foundation, the NSF under Grant Nos. DMR-0820382 and DMR-1005880, NASA NEPP, and DTRA. J. Hicks and E. Kenyon would like to acknowledge support from the NSF GRFP under Grant No. DGE-0644493.

References

1. C. Berger, Z. Song, T. Li, X. Li, Y. Ogbazghi, R. Feng, Z. Dai, N. Marchenkov, E. H. Conrad, P. N. First, and W. A. de Heer, *J. Phys. Chem. B* **108** (2004).

J. S. Moon, D. Curtis, M. Hu, D. Wong, C. McGuire, P. M. Campbell, G. Jernigan,
2. J. L. Tedesco, B. VanMil, R. Myers-Ward, C. Eddy, Jr., and D. K. Gaskill, IEEE ELECTRON DEVICE LETTERS, VOL. 30, NO. 6, JUNE 2009

3. Y.-M. Lin, C. Dimitrakopoulos, K. A. Jenkins, D. B. Farmer, H.-Y. Chiu, A. Grill, and Ph. Avouris, *Science* **327** (2010).
4. J. S. Moon, D. Curtis, S. Bui, M. Hu, D. K. Gaskill, J. L. Tedesco, P. Asbeck, G. G. Jernigan, B. L. VanMil , R. L. Myers-Ward, C. R. Eddy, Jr., P. M. Campbell, and X. Weng, IEEE ELECTRON DEVICE LETTERS, VOL. 31, NO. 4, APRIL 2010
5. C. M. Dozier and D. B. Brown, *IEEE Trans. Nucl. Sci.* **27** (1980).
6. C. D. Cress, J. J. McMorrow, J. T. Robinson, A. L. Friedman, and B. J. Landi, *IEEE Trans. Nucl. Sci.* **57** (2010).
7. S. A. Vitusevich, V. A. Sydoruk, M. V. Petrychuk, B. A. Danilchenko, N. Klein, A. Offenhäusser, A. Ural, and G. Bosman, *J. Appl. Phys.* **107** (2010).
8. S. Y. Zhou, Ç. Ö. Girit, A. Scholl, C. J. Jozwiak, D. A. Siegel, P. Yu, J. T. Robinson, F. Wang, A. Zettl, and A. Lanzara, *Phys. Rev. B* **80** (2009).
9. W. A. de Heer, C. Berger, M. Ruan, M. Sprinkle, X. Li, Y. Hu, B. Zhang, J. Hankinson, and E. H. Conrad, *Nat. Acad. Sci. Proc.* (in print).
10. M. Guggisberg, M. Bammerlin, Ch. Loppacher, O. Pfieffer, A. Abdurixit, V. Barwich, R. Bennewitz, A. Baratoff, E. Meyer, and H.-J. Güntherodt, *Phys. Rev. B* **61** (2000).
11. C. Berger, Z. Song, X. Li, X. Wu, N. Brown, C. Naud, D. Mayou, T. Li, J. Hass, A. N. Marchenkov, E. H. Conrad, P. N. First, and W. A. de Heer, *Science* **26** (2006).
12. T. Ohta, A. Bostwick, J. L. McChesney, T. Seyller, K. Horn, and E. Rotenberg, *Phys. Rev. Lett.* **98** (2007).
13. F. Tuinstra and J. L. Koenig, *J. Chem. Phys.* **53** (1970).
14. R. J. Niemanich and S. A. Solin, *Phys. Rev. B* **20** (1979).
15. C. Faugeras, A. Nerrière, M. Potemski, A. Mahmood, E. Dujardin, C. Berger, and W. A. de Heer, *Appl. Phys. Lett.* **92** (2008).

16. D. Q. Yang and E. Sacher, *Langmuir* **22** (2006).

17. T. I. T. Okpalugo, P. Papakonstantinou, H. Murphy, J. McLaughlin, and N. M. D. Brown, *Carbon* **43** (2005).

18. S. Kundu, Y. Wang, W. Xia, and M. Muhler, *J. Phys. Chem. C* **112** (2008).

Figure Captions

Figure 1. Non-contact AFM image of a Hall bar (dashed line outline) before (a) and after (b) irradiation. The arrows point to an areas where the top layers of graphene peeled from the surface along a narrow path. The Hall bars are 10 μm wide. (c) Height profile of the solid bar in

Fig.'s 1(a) and (b), which goes over one such peeled path in the latter case. (d) Ratio of mobility (μ), carrier density (n) and resistivity (ρ) values of all Hall bars tested before and after irradiation with the vertical line repsenting the median value. Figure 2. (a) Background-subtracted Raman spectroscopy of bulk epitaxial graphene before (top) and after (bottom) irradiation. The G and 2D peaks are normalized independently to be the same integrated intensity. (b) C1s XPS of the same general area before (top) and after (bottom) irradiation, the former being fitted to two Lorentzians and the latter being fitted to six. The curves are normalized to have the same integrated graphene intensity and shifted to have the same graphene peak position (284.5 eV).

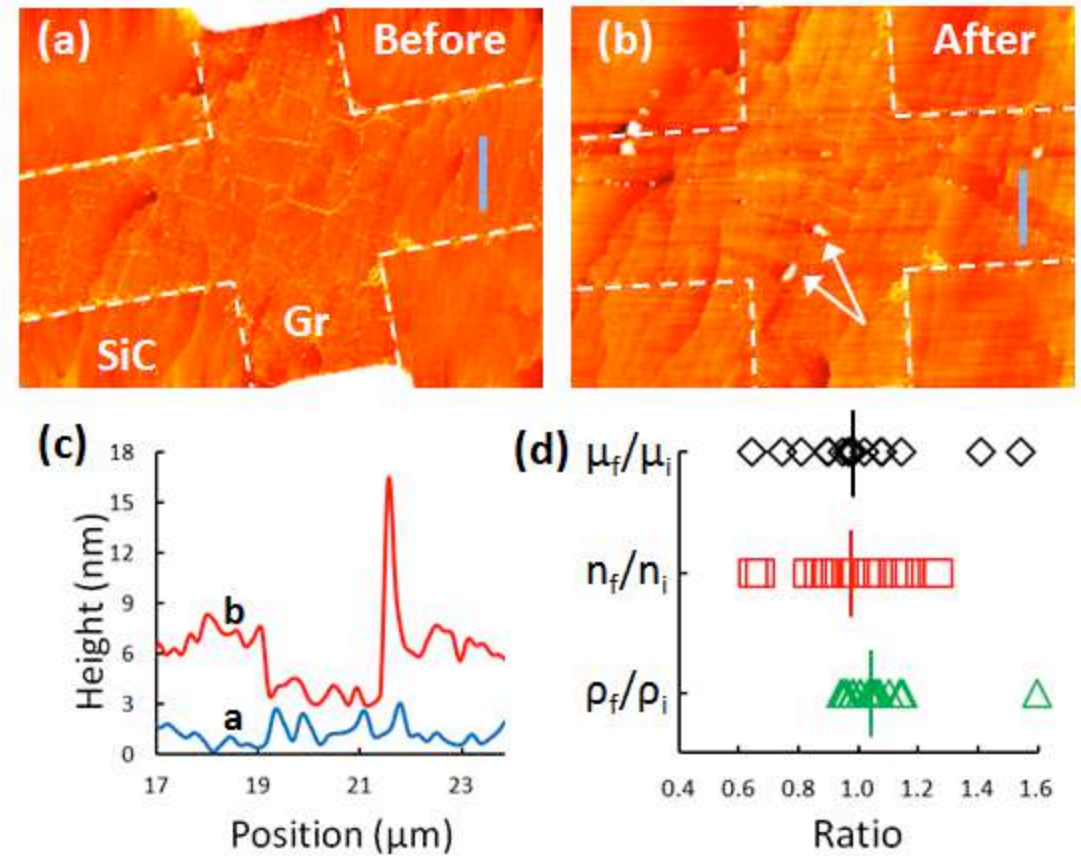

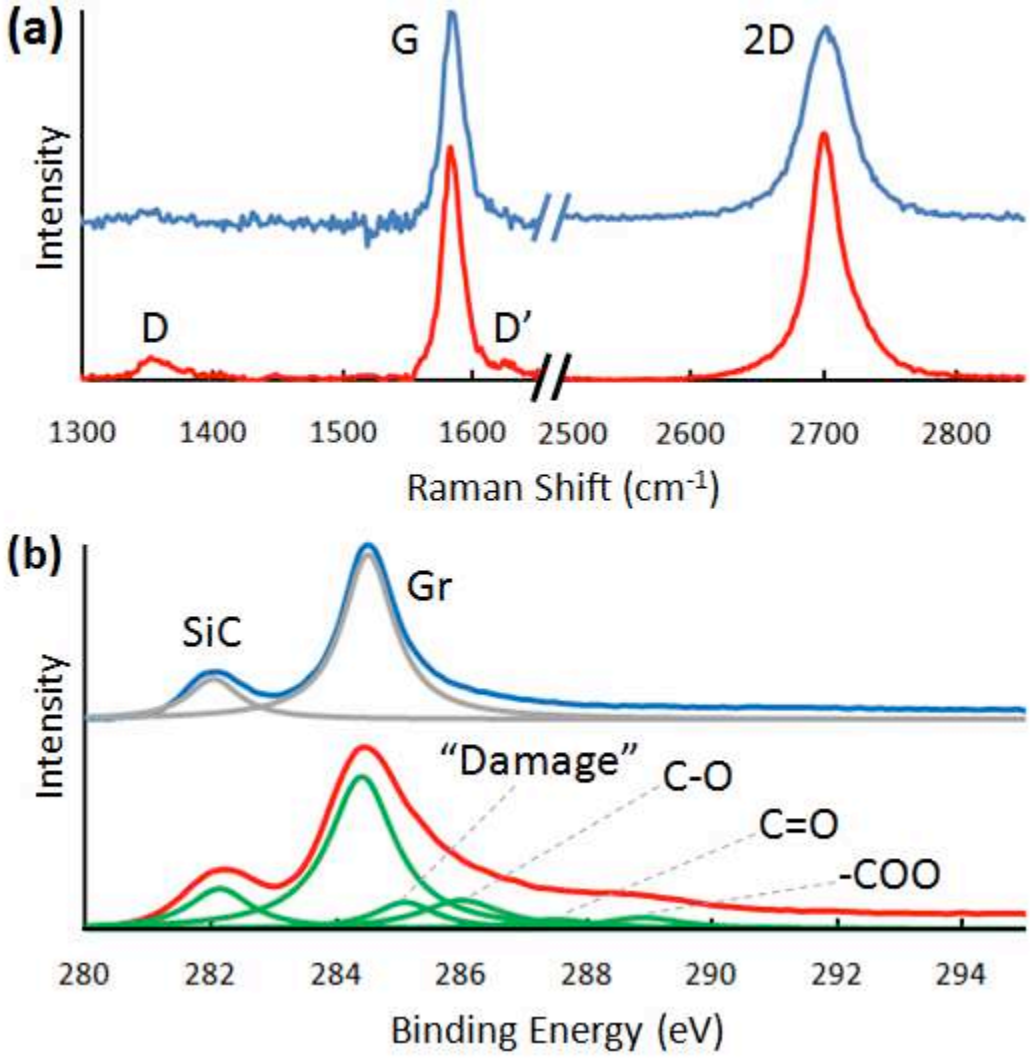
(a)
G
2D
Intensity
D
D'
1300
1400
1500
1600
2500
2600
2700
2800
Raman Shift (cm-1)
(b)
Gr
SiC
Intensity
"Damage"
C-O
C=O
-COO
280
282
284
286
288
290
292
294
Binding Energy (eV)